JOURNAL OF PETROLOGY | VOLUME 47 | NUMBER 4 | PAGES 791–800 | 2006 | doi:10.1093/petrology/egi094

Melt–Solid Dihedral Angles of Common Minerals in Natural Rocks

M. B. HOLNESS*

DEPARTMENT OF EARTH SCIENCES, UNIVERSITY OF CAMBRIDGE, DOWNING STREET, CAMBRIDGE CB2 3EQ, UK

RECEIVED MAY 5, 2005; ACCEPTED NOVEMBER 17, 2005; ADVANCE ACCESS PUBLICATION DECEMBER 20, 2005

The melt–solid dihedral angle has been measured in a range of igneous rock types, ranging in composition from picrite, through basalt, phonolite, andesite and rhyolite, for the minerals quartz, leucite, plagioclase, olivine, amphibole and clinopyroxene. Populations of up to 104 true 3-D angles were measured in each sample using a universal stage mounted on an optical microscope. The median and standard deviation of the angle populations for each mineral are distinct (plagioclase ~25°, with standard deviation (SD) 11°; clinopyroxene ~38°, with SD 14°; olivine ~29°, with SD 13°; quartz ~18°, with SD 9°; leucite ~20°, with SD 11°), with no control by either melt composition or degree of approach of the grains to their equilibrium shapes.

KEY WORDS: *dihedral angle, textural equilibrium, universal stage*

INTRODUCTION

The angle subtended at the junctions of two solid grains in textural equilibrium with a fluid phase, the fluid–solid–solid dihedral angle, provides important information about the physical and chemical properties of a two-phase system. The angle is controlled by the relative magnitudes of the energy of the grain boundary and that of the fluid–solid interfaces, via the governing equation:

$$\sum_{i=1}^{3}(\gamma_i \mathbf{t}_i + \frac{\partial \gamma_i}{\partial \mathbf{t}_i}) = 0$$

where γ_1, γ_2, γ_3 are the three interfacial energies, $\mathbf{t}_i$ is the vector in the plane of the ith surface, normal to the line of intersection of the surfaces and pointing away from this line, and $\partial\gamma_i/\partial\mathbf{t}_i$ is a vector perpendicular to $\mathbf{t}_i$ and to the line of intersection (Herring, 1951*a*). This equation defines the orientation of the interfaces at a three-grain junction or a pore corner, and hence the dihedral angle. The tangential component of this equation acts to minimize the surface area, whereas the normal component acts to rotate the interface towards an orientation with a lower interfacial area. Hence, in general, the dihedral angle varies with crystalline orientation (Herring, 1951*a*; Laporte & Provost, 2000*a*). For isotropic systems, in which the interfacial energy is constant regardless of the orientation of the interface, the normal term vanishes. The resultant simplified form of this equation, applicable only to isotropic systems, was first presented by Smith (1948).

The variation of dihedral angle with pressure, temperature and fluid composition is controlled by the composition of the layer of adsorbed species on both the grain boundary and the fluid–solid interface (Holness, 1993). Thus, determination of dihedral angle in P–T–X space can be used to constrain the nature and adsorption density of species at the interface (Holness, 1993; Holness & Lewis, 1997).

The dihedral angle is a prime control on the connectivity of the fluid phase, and hence the permeability of the fluid-bearing rock. As a first approximation (neglecting the effects of crystalline anisotropy), systems with a fluid–solid dihedral angle $\leq 60°$ contain a fully interconnected network of fluid-filled channels on three-grain junctions, stable even for vanishingly low porosities (Smith, 1964; Bulau *et al.*, 1979; Watson, 1982). Realistic systems, with some anisotropy of interfacial energies, have a percolation threshold, at porosities of a few percent, even for median angles $\leq 60°$ (e.g. Minarik & Watson, 1995; Wark & Watson, 1998).

Given the importance of the dihedral angle to rock properties, there have been numerous attempts to quantify the dihedral angle for melt-bearing systems of geological interest [see Laporte & Provost (2000*b*) for a

*E-mail: marian@esc.cam.ac.uk

comprehensive list to that date; also Wark *et al.* (2003) and Maumus *et al.* (2004)]. Many of the data are contradictory, with wide ranges of reported angles for essentially the same systems, although the great majority are <60°. All the published data are experimental determinations of angles in either synthetic or natural systems, and comprise populations of angles measured on randomly oriented 2-D sections through the melt-bearing aggregate. The median value of such a population is close to the true, 3-D, dihedral angle for an isotropic system in which the angle is single-valued (Harker & Parker, 1945; Riegger & Van Vlack, 1960). However, systems of interest to geologists are more or less anisotropic (e.g. Kretz, 1966; Vernon, 1968; Laporte 1994; Schäfer & Foley, 2002), and a range of true 3-D angles is to be expected (Herring, 1951*a*; Laporte & Provost, 2000*a*). Apart from the preliminary results of Holness *et al.* (2005), there are no published direct measurements of the range of true 3-D angles in melt-bearing rocks, and consequently no assessments of the relative extent of anisotropy of these materials.

In this contribution I report the results of a series of measurements of true, 3-D, melt–solid dihedral angles for common rock-forming minerals forming enclaves, crystal clots and glomerocrysts in natural volcanic rocks. The new data suggest that melt–solid median angles are generally <40° and are not sensitive to melt composition. The effects of anisotropy result in standard deviations of 8–15° about the mean.

PREVIOUS WORK

In addition to the stabilization of a range of equilibrium 3-D dihedral angles, anisotropy of interfacial energies results in planar interfaces (Wulff, 1901; Herring, 1951*b*). The equilibrium shape of an isolated grain of an anisotropic mineral, suspended in an isotropic medium, thus differs from the sphere expected for a grain of a perfectly isotropic substance. This shape may include facets, which either coexist with curved surfaces, or cover the entire surface area of the grain depending on the extent of anisotropy (Herring, 1951*b*). The anisotropy of a substance can thus be determined from the extent of departure of an isolated grain from a spherical shape.

Despite its importance in controlling rock properties, the extent of surface energy anisotropy in common rock-forming minerals is not well known. Qualitative assessments of the relative extent of anisotropy in melt-bearing aggregates have been made using the extent of development of planar melt–solid interfaces (Laporte, 1994; Laporte & Watson, 1995; Lupulescu & Watson, 1995; Cmíral *et al.*, 1997), although detailed assessments of equilibrium grain shapes are rare (Kretz, 1966; Vernon, 1968; Laporte, 1994; Saiki *et al.*, 2003). A study of the anisotropy of mineral surfaces wetted by silicate melts has been presented by Schäfer & Foley (2002), who concluded that anisotropy increases in the order spinel < orthopyroxene < olivine < clinopyroxene. Apparently fully equilibrated grains of even relatively anisotropic minerals such as amphibole (Laporte & Watson, 1995; Lupulescu & Watson, 1999; Vernon, 1999; Holness *et al.*, 2005) develop significant areas of curved surface in contact with silicate melts, showing that the anisotropy of common geological materials is not sufficient to stabilize completely faceted grains. Fully faceted grains of such minerals are, thus, out of textural equilibrium, with shapes controlled more by growth processes than by minimization of interfacial energy.

There is little information on the range of dihedral angles to be expected for texturally equilibrated rock-forming anisotropic minerals. Kretz (1966) and Vernon (1968, 1970) presented standard deviations for solid–solid dihedral angle populations for granulite-grade rocks, Holness *et al.* (2005) presented some preliminary data for melt–solid angles, and Laporte & Provost (2000*a*) presented a calculated standard deviation for melt-bearing feldspar aggregates.

ANALYTICAL METHODS

For anisotropic materials, sophisticated statistical techniques are required to extract the range of true equilibrium angles from populations of dihedral angles measured on 2-D sections (e.g. Jurewicz & Jurewicz, 1986; Laporte & Provost, 2000*a*). However, for sufficiently coarse-grained samples (which include many natural materials of interest), direct measurement of the true dihedral angle can be achieved using a universal stage mounted on an optical microscope, thus permitting direct assessment of the true range of angles and consequently the significance of anisotropy on melt topology (e.g. Kretz, 1966; Vernon, 1968, 1970, 1997; Holness, 2005; Holness *et al.*, 2005).

I used a four-axis Leitz Wetzlar universal stage, mounted on a Leitz Wetzlar Ortholux microscope, with a magnification of ×300. The universal stage permits up to 80° rotation of the thin section from the horizontal, and allows accurate measurement of most of the dihedral angles present in the sample, with an error on each measurement of a few degrees. I measured between 32 and 104 angles in each sample, using trial and error to align all three boundaries at three-grain junctions so that they were parallel to the line of sight. Parallelism resulted in the boundaries being at their most sharply defined, and the optimum position was estimated by eye. Measurement of dihedral angles was made from pairs of phenocrysts joined by a well-defined grain boundary, and from coherent crystal clots displaying well-defined grain boundaries. Up to 10 thin sections were made of

Table 1: Details of the sample set

Sample	Solid	Liquid	*n*	Mean	Median	SD	Notes
13485	plagioclase	inninmorite (64 wt % SiO_2)	60	25·8	23	10·2	Mull, Scotland; Anderson & Radley (1915)
13483	plagioclase	inninmorite (62 wt % SiO_2)	80	26·9	25	10·9	Mull, Scotland; Anderson & Radley (1915)
Iceland	plagioclase	basalt	74	27·6	26	11·6	Theistareykir; McClennan *et al*. (2003)
P	plagioclase	rhyolite	60	25·8	24	11·5	Arran, Scotland; Cambridge Teaching Collection
30440	plagioclase	rhyolite	40	28·3	25·5	10·7	Arran, Scotland
13483	clinopyroxene	inninmorite (62 wt % SiO_2)	61	38·7	38	13·4	Mull, Scotland; Anderson & Radley (1915)
13485	clinopyroxene	inninmorite (64 wt % SiO_2)	85	38·7	39	13·4	Mull, Scotland; Anderson & Radley (1915)
K96-022	clinopyroxene	phonolite	100	39·3	37	14·8	Kula, Turkey; Holness & Bunbury (2005)
K96-005	clinopyroxene	phonolite	91	38·1	38	13·8	Kula, Turkey; Holness & Bunbury (2005)
151023	clinopyroxene	basalt	50	38·6	37·5	13·0	Mammoth Lakes, USA
K96-022	amphibole	phonolite	104	31	28	14·4	Kula, Turkey; Holness & Bunbury (2005)
79596	olivine	picrite	32	28·5	29	9·05	Picrite dyke, Scotland
Iceland	olivine	basalt	55	29·3	29	12·7	Theistareykir; McClennan *et al*. (2003)
M9	olivine	picrite	40	30·5	28·5	14·1	Picrite dyke, Rum, Scotland; Upton *et al*. (2002)
151023	olivine	basalt	41	33·8	27	14·7	Mammoth Lakes, USA
K96/069	olivine	phonolite	60	29·7	29	11·9	Kula, Turkey; Holness & Bunbury (2005)
65832	quartz	rhyolite	60	19·6	19	9·7	Arran, Scotland
AGS66-13	quartz	rhyolite	72	20·7	18	9·8	Arran, Scotland; Cambridge Teaching Collection
P	quartz	rhyolite	69	19·8	18·5	9·2	Arran, Scotland; Cambridge Teaching Collection
S	quartz	rhyolite	80	19·0	18	9·1	Arran, Scotland; Cambridge Teaching Collection
29668	leucite	tephrite	80	22·5	20	10·9	1889 flow, Vesuvius
29669	leucite	tephrite	79	22·5	20	10·4	1889 flow, Vesuvius

Sample numbers in bold type are those from the Harker Collection. Others are from the author's collection, from the Cambridge teaching collection, or on loan. References are given for further description of the samples (including mineral and liquid compositions) where possible. *n*, number of measurements; SD, standard deviation. The complete datasets are available as Electronic Appendix 1 at http://www.petrology.oupjournals.org/.

individual samples with rare crystal clots, to obtain a statistically meaningful value of standard deviation.

CHOICE OF SAMPLES

The set of samples is dominated by porphyritic lavas from the Harker Collection (housed in the Department of Earth Sciences, University of Cambridge). Care was taken to choose lavas in which the phenocrysts show no signs of resorption or reaction on the margins, and which have at least some surface rounding, indicating approach to equilibrium. An additional criterion was a fine-grained or glassy groundmass. The sample set comprises a range of liquid compositions from picrite, through basalt, to phonolite and rhyolite. Several samples contain two phenocryst minerals. Details of the samples, with brief indications of mineral and liquid compositions (together with references for more detailed compositional information), are given in Table 1.

Further samples are from the rift-related, Quaternary, Kula Volcanic Province in western Turkey, where several of the monogenetic, tephrite–basanite volcanic cones contain abundant crystal-rich nodules derived from a crystal mush that developed on the margins of the magma plumbing system during fractionation of earlier erupted lavas (Holness & Bunbury, 2005). The nodule population is dominated by almost monomineralic, phonolitic glass-bearing, amphibole cumulates, some of which contain variable amounts of clinopyroxene and apatite.

Other samples of glass-bearing, crystal-rich, nodules were collected from the basaltic Borgahraun flow from the Theistareykir segment of the Northern Volcanic Zone of Iceland. The crystal-rich nodules are small (<1 cm diameter) and include gabbros, wehrlites and troctolites; details have been given by Maclennan *et al.* (2003). Some dihedral angle measurements from these nodules have been reported previously by Holness *et al.* (2005).

Amphibole

Fresh amphibole phenocrysts are rare in lavas, as a result of dehydration breakdown on ascent. Only one suitable

sample was found. This is a nodule from the Kula Volcanic Province, dominated by pristine kaersutitic amphibole set in vesicular phonolitic glass (Fig. 1a).

Clinopyroxene

Pigeonite phenocrysts in an inninmorite [this local name, originating with Anderson & Radley (1915), refers to a fine-grained andesitic to dacitic rock containing phenocrysts of calcic plagiclase and pigeonite] form glomerocrystic clumps of non-faceted rounded grains (Fig. 1b). Titanaugite in the glassy nodules of the Kula Volcanic Province forms a framework of partially faceted grains (Fig. 1c). A further sample is a basalt from the Mammoth Lakes area of California, in which diopsidic clinopyroxene forms almost fully faceted phenocrysts (Fig. 1d).

Olivine

Olivine–melt dihedral angles were measured in a glassy nodule within a basaltic flow from Theistareykir. The nodules comprise a low-porosity aggregate of rounded olivine grains (Fig. 1e). A further sample is from an olivine-phyric (Fo_{90}) picritic dyke on the Isle of Rum, known as M9 (McClurg, 1982; Upton *et al.*, 2002), in which olivine forms partially faceted phenocrysts (Fig. 1f). Measurements were also made of faceted olivine phenocrysts in a picritic dyke from Applecross, Scottish Highlands, in the basalt from the Mammoth Lakes area of California (Fig. 1d), and in olivine-rich phonolitic glass-bearing nodules from Kula.

Leucite

Leucite–glass angles were measured in the abundant, monomineralic, polycrystalline clumps of leucite in glassy tephrite from the 1889 flow on the SE side of Mount Vesuvius (Fig. 1g).

Plagioclase

The sample set includes clumps of partially faceted plagioclase phenocrysts associated with pigeonite in the inninmorites (Fig. 1h), and plagioclase-dominated, glass-bearing, nodules in the Theistareykir basalts (Fig. 1i). Further measurements were made on rounded plagioclase glomerocrysts in pitchstones from the Isle of Arran.

Quartz

Quartz phenocrysts are found only in highly silicic lavas such as rhyolites. Measurements were made on quartz-phyric glassy rhyolites containing glomerocrysts of smoothly rounded, only rarely faceted, quartz (Fig. 1j).

RESULTS

The mean, median and standard deviation, together with the size of the measured population, are given for each sample in Table 1. The full dataset (Electronic Appendix 1) is available for downloading from the *Journal of Petrology* web site at http://www.petrology.oupjournals.org. Representative frequency plots are given in Fig. 2. The range of mean, median and standard deviation is shown in Fig. 3. It was found that the mean and median changed by $<1^\circ$ for successively larger populations of measurements for populations greater than about 25 observations. However, stabilization of the standard deviation (i.e. to within 1°) requires populations of >50 measurements. The error on the standard deviation is likely to be $\pm 3^\circ$, and that of the mean and median value is likely to be $\pm 1^\circ$. The mean is generally higher than the median, and the populations are slightly positively skewed relative to a symmetrical distribution. The kurtosis of each population varies from $-0{\cdot}9$ to $2{\cdot}6$, with most populations being peaked relative to a normal distribution.

The melt–solid dihedral angle population for each mineral phase is distinct (Fig. 3). For each mineral, the mean and median vary within a maximum range of 3° (with the exception of olivine, for which the mean varies by up to 5°), regardless of the composition of the melt. The standard deviation also generally varies by only 3° for each mineral, although there is a single result for olivine with a very low standard deviation. This outlier represents a population of 34 measurements and its standard deviation is most probably too low. The result is included to show that the mean and median of this population are indistinguishable from those determined from larger populations.

The lowest melt–solid dihedral angles occur in quartz aggregates, with increasing angles observed for leucite, plagioclase, olivine, amphibole and clinopyroxene. In general, the lowest standard deviations, and thus the lowest degree of anisotropy, are found for the minerals with the lowest mean and median dihedral angles. The least anisotropic system is quartz–melt, with leucite and plagioclase displaying a greater extent of anisotropy. The most anisotropic minerals are olivine, amphibole and clinopyroxene, for which the standard deviations are indistinguishable.

There is no effect of the degree of rounding of the phenocrysts on either mean, median or standard deviation. This is particularly well illustrated by clinopyroxene, for which the samples range from almost fully faceted to completely rounded grains (Fig. 1b–d).

DISCUSSION AND CONCLUSIONS

The relative order of increasing anisotropy of quartz $<$ leucite $=$ plagioclase $<$ olivine $=$ clinopyroxene $=$

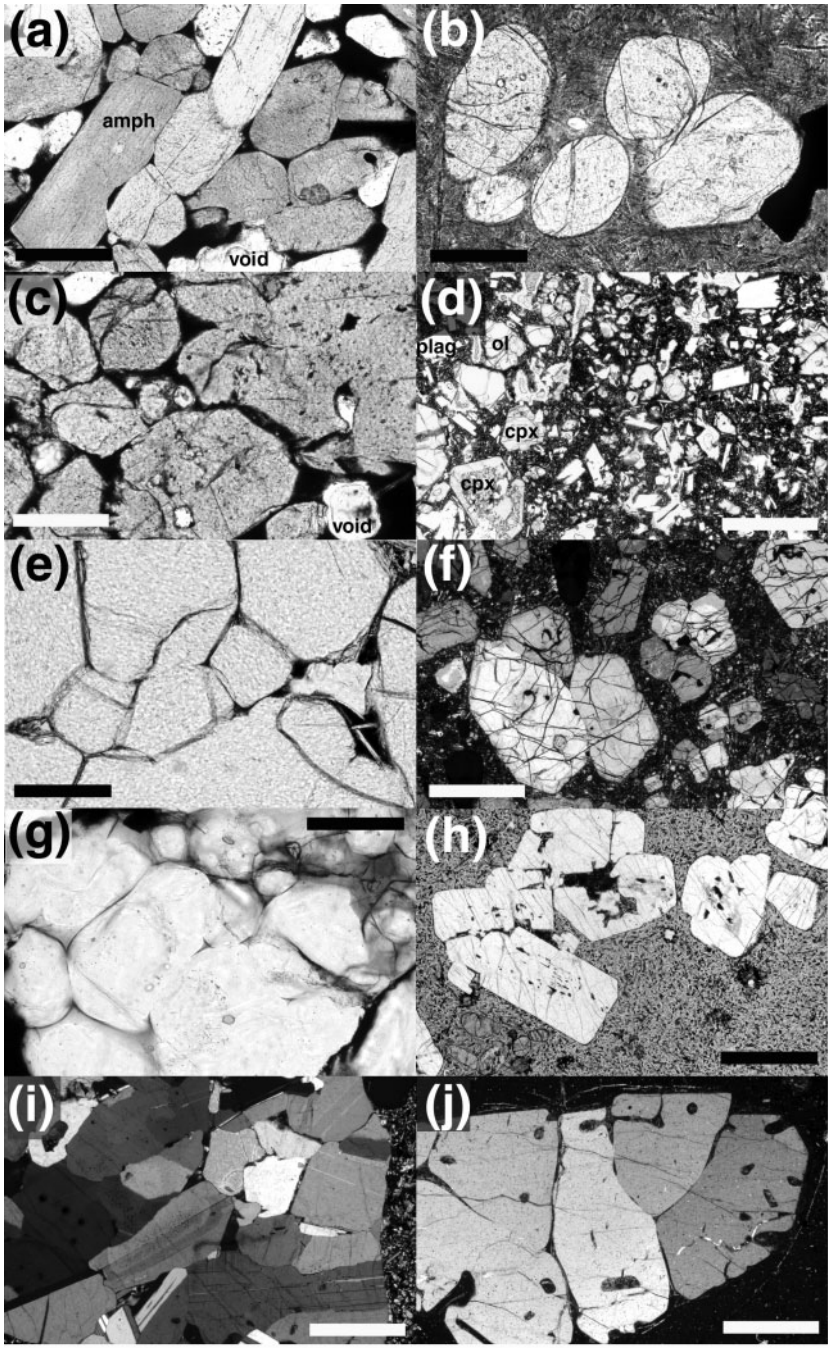

Fig. 1. Photomicrographs of samples used for dihedral angle measurements. Details of measurements are presented in Table 1. (a) K96-021, nodule in tephrite from Kula Volcanic Province, Turkey. Kaersutitic amphibole set in vesicular glass (black). Note rounding of the {110} faces. Scale bar represents 200 μm. (b) 13485, inninmorite sill (term defined in the text), Mull, Scotland. Pigeonite glomerocrysts in fine-grained matrix. Note the rounded shape of the pyroxene. Scale bar represents 1 mm. (c) K96-022, nodule in tephrite from Kula Volcanic Province, Turkey. Titanaugite in vesicular glass (black). Scale bar represents 200 μm. (d) 151023, basalt from Barrow Pit, Mammoth Lakes, USA. Phenocrysts of olivine, plagioclase and clinopyroxene, all showing prominent facets formed during growth. Scale bar represents 1 mm. (e) Dunitic nodule from Theistareykir basalt. Note the low porosity (black glass). Scale bar represents 200 μm. (f) M9, olivine-phyric picrite dyke from Rum, Scotland, with glomerocrysts of partially rounded olivine. Scale bar represents 1 mm. (g) 29669, glomerocryst of leucite in tephrite, Vesuvius, Italy. Note the partially faceted grains set in pale brown glass. Scale bar represents 200 μm. (h) 13485, inninmorite sill, Mull, Scotland. Glomerocrysts of partially faceted plagioclase set in fine-grained groundmass. A clump of rounded pigeonite crystals is in the lower left-hand corner of the image [shown in (b)]. Scale bar represents 1 mm. (i) Troctolitic nodule from Theistareykir basalt, with well-sintered, low-porosity plagioclase aggregates. The pore space is filled with glass and fine-grained crystalline material. Scale bar represents 1 mm. (j) 65832, pitchstone from Arran, Scotland. Well-sintered aggregate of quartz, with porosity filled with fine-grained groundmass. The surrounding matrix is glassy. Scale bar represents 1 mm.

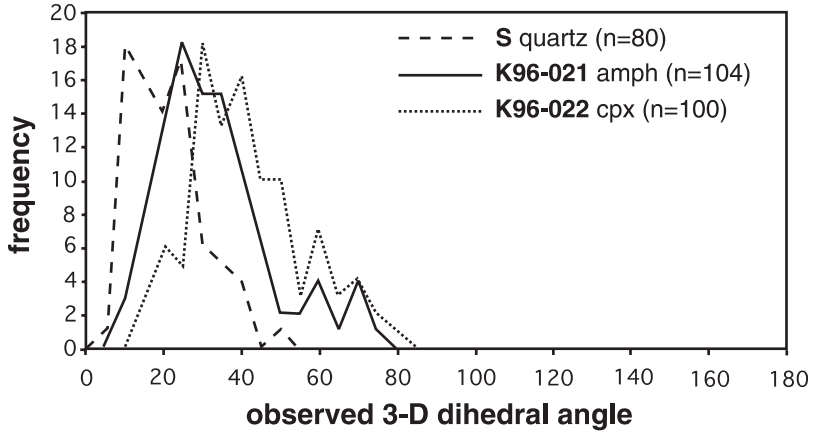

Fig. 2. Frequency plots for three representative samples. The number of observations for each population is given by *n*. (For further details see Table 1.)

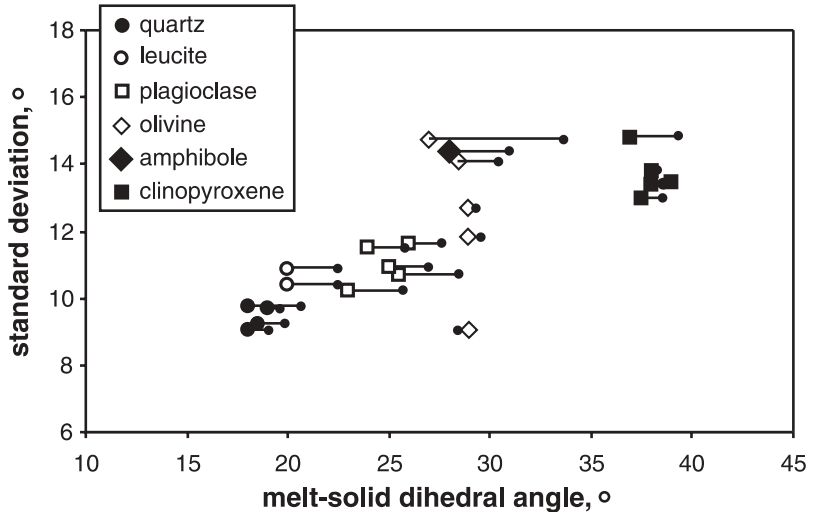

Fig. 3. Mean, median and standard deviations of true 3-D melt–solid–solid dihedral angles in natural rocks. The large symbols give the median values of the populations, and the coupled small dot gives the mean. For the great majority of the samples the mean is higher than the median, and the population has a slight positive skewness.

amphibole differs somewhat from the results of Schäfer & Foley (2002), who found that olivine was less anisotropic than clinopyroxene. This suggests that the standard deviation for some of the olivine samples described here may be slightly too high, perhaps as a result of the presence of a small number of non-equilibrated boundaries. To a first approximation, the order of increasing anisotropy presented here is reflected in the relative magnitudes of the birefringence for these minerals.

Some of the quartz and plagioclase phenocrysts in the sample suite show embayments, perhaps indicative of resorption (Fig. 1j). However, Vernon (2004) suggested that such textural features may be partially equilibrated dendrites in the case of quartz. The melt–solid dihedral angles in these samples were mainly measured in enclosed pores, which are unlikely to have been affected by dissolution (e.g. Fig. 1 h–j). I suggest that the observed quartz–melt and plagioclase–melt angle populations represent textural equilibrium. Evidence that dissolution did not control the grain shapes of the non-embayed phenocrysts (e.g. Fig. 1a and b) is provided by smoothly curved grain surfaces, which show no break in slope as two-grain junctions are approached. Such constant mean curvature is a requirement of textural equilibrium for isotropic materials (Bulau *et al.*, 1979), and is unlikely to occur for grains that have been partially resorbed.

The sample suite displays a range of grain shapes for each of the minerals examined. This is particularly well illustrated for clinopyroxene (Fig. 1b–d). I suggest that the range in shapes results from a varying balance between

the two controls of grain growth and interfacial energy minimization. Growth results in planar facets, which are then rounded during an approach to textural equilibrium. The wide variation in approach to the rounded equilibrium shape observed in the sample suite reported here would then be caused by differences in the relative rates of crystal growth and textural equilibration, as a result, perhaps, of differences in cooling or ascent rates of the individual magma systems. The rounded form of the pigeonite in Fig. 1b is admittedly very rare. I suggest that this rarity results from the dominant role of crystal growth in erupted magmas: the generally observed euhedral shape of pyroxene phenocrysts (e.g. Fig. 1d) is due to growth control on crystal shape rather than a faceted equilibrium shape.

If it is true that the equilibrium shape of clinopyroxene is dominated by curved surfaces, then given the relatively high standard deviation for the equilibrium clinopyroxene–melt angles (and hence the relatively anisotropic nature of pyroxene) this suggests that the equilibrium shape of amphibole (with a similar standard deviation, Fig. 3) is not dominated by planar facets, but is similarly rounded, consistent with Fig. 1a. In this Kula enclave, the amphibole grains are variably elongate, although they exhibit significant rounding of the {110} faces. The elongate amphibole prisms common to many experimental charges (and many natural examples) are thus most probably a result of growth control, and if further time were available, would attain a shape similar to those for clinopyroxene (Fig. 1b).

The populations of angles obtained from well-rounded phenocrysts are indistinguishable from those obtained from more euhedral grains. This is consistent with the conclusions of Laporte & Watson (1995) and Holness *et al.* (2005) that the equilibrium dihedral angle is achieved faster than the equilibrium shape, especially for large crystals. This suggests that the dihedral angle may control melt topology and connectivity even in rocks with grain-scale textures far from equilibrium.

The pressure and temperature conditions under which the phenocrysts, glomerocrysts and enclaves of the sample suite equilibrated with their host are not known, but are likely to cover a wide range. Given this, and the wide range of liquid compositions represented in the sample suite, the similarity of the dihedral angle populations for each mineral is noteworthy. The absence of an effect of melt composition on dihedral angle is consistent with the experimental results of Laporte (1994) for quartz–melt, and also with the conclusions of Laporte & Provost (2000*b*) for olivine–melt. If the published values for olivine carbonatite (Hunter & McKenzie 1989; Watson *et al.*, 1990), and olivine komatiite (Walker *et al.*, 1988) are correct, this would suggest olivine–melt dihedral angles remain at ~30° in liquids ranging in composition from komatiite, through carbonatite, basalt and phonolite to picrite. The only exception to this is the unusual SiO_2-rich mantle melt investigated by Maumus *et al.* (2004). Such constancy of melt–solid dihedral angle across a wide spectrum of liquid compositions also appears to hold for plagioclase and clinopyroxene.

The lack of compositional control is surprising. In simple binary silicate systems, such as diopside–anorthite, there is a clear relationship between solid–solid–melt angle with composition, analogous to those observed in binary metallic alloys [Ikeda *et al.* (2002): their results also show a related variation with temperature]. The answer may lie in the greater complexity of natural systems. Interfacial energies are strongly controlled by adsorption of chemical species from the liquid, and it is possible that selective adsorption [as shown by the results of Wanamaker & Kohlstedt (1991)] may counteract any tendencies towards a systematic change of interfacial energy with liquid composition.

The median values of the dihedral angle populations are compared with those in the published literature in Fig. 4. The amphibole datum is in agreement with that of Vicenzi *et al.* (1988) and Laporte & Watson (1995); the quartz data are in agreement with the results of Laporte (1994) and Laporte & Vielzeuf (1994); the plagioclase data are close to those of Laporte *et al.* (1997) and Holness *et al.* (2005); and the olivine data are close to those of Bulau (1982) and Holness *et al.* (2005). The clinopyroxene data are similar to the top of the range of values of enstatite–melt angles obtained by von Bargen & Waff (1988), consistent with the results of Schäfer & Foley (2002), who found that enstatite is less anisotropic (and thus likely to have a lower median dihedral angle; Fig. 3) than diopside.

A significant number of previously published medians differ from those reported here, with many being much higher. An exception to this is the low olivine-basalt angle reported by Cmíral *et al.* (1997); however, Laporte & Provost (2000*a*) considered the result of Cmíral *et al.* (1997) to be biased towards low angles. The large range of previously reported values merits some discussion, given the new results, which show that it cannot plausibly be accounted for by differences in melt composition or in composition of solid solutions (or, probably, by differences in pressure nor temperature).

Overestimation of a dihedral angle may be due to several factors. Laporte (1994) and Laporte & Provost (2000*a*) pointed out that the grain size of experimental charges is generally small, prohibiting accurate measurement of the angle in the immediate vicinity of the pore corner. A further contributory factor may be the influence of crystal growth during an incompletely equilibrated charge, which results in an increase of median angle towards a maximum of ~60° (Elliott *et al.*, 1997; Holness *et al.*, 2005).

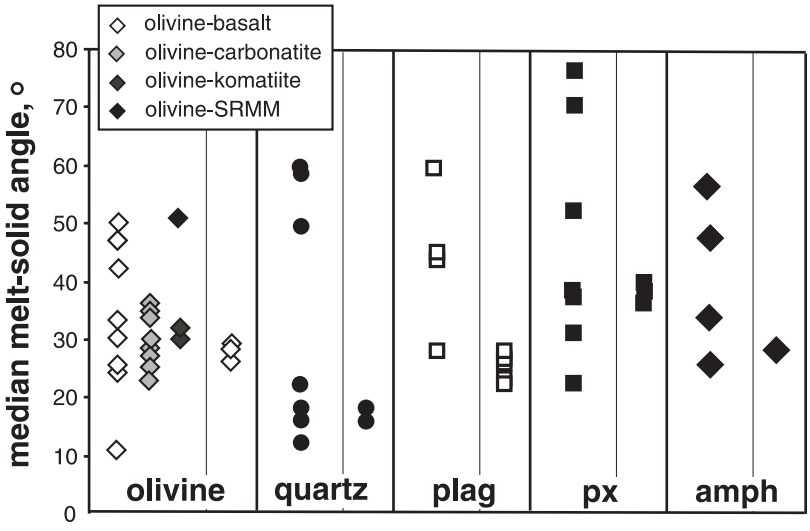

Fig. 4. Published median values of experimentally determined melt–solid–solid dihedral angles, compared with those reported here and by Holness *et al.* (2005) (shown in the right-hand box for each mineral). Olivine-basalt data from Waff & Bulau (1979), Bulau (1982), Fujii *et al.* (1986), Jurewicz & Jurewicz (1986), Toramaru & Fujii (1986) and Cmíral *et al.* (1998). Olivine-carbonatite data from Hunter & McKenzie (1989) and Watson *et al.* (1990). Olivine-komatiite data from Jurewicz & Jurewicz (1986) and Walker *et al.* (1988). Olivine–SiO_2-rich mantle melt (SRMM) datum from Maumus *et al.* (2004). Orthopyroxene-basalt data from Fujii *et al.* (1986; calculated), Toramaru & Fujii (1986) and Von Bargen & Waff (1988). It should be noted that the data for this study refer to a monoclinic pyroxene. Amphibole–melt data from Laporte & Watson (1985), Vicenzi *et al.* (1988) and Lupulescu & Watson (1994, 1995, 1999). Plagioclase–melt data from Jurewicz & Watson (1985; alkali feldspar), Vicenzi *et al.* (1988), Longhi & Jurewicz (1995) and Laporte *et al.* (1997). Quartz–melt data from Jurewicz & Watson (1985), Laporte (1994), Laporte & Vielzeuf (1994) and Holness (1995).

ACKNOWLEDGEMENTS

I am indebted to Steve Laurie for facilitating access to the Harker Collection, and to Henry Emeleus and Dan McKenzie for loan of samples. Mike Cheadle and David Wark are thanked for stimulating discussions. This research was funded in part by the European Community's Human Potential Programme under contract HPRN-CT-2002-000211 [EUROMELT]. Ron Vernon, Didier Laporte and Dougal Jerram are thanked for extremely constructive reviews of an earlier version of the manuscript.

SUPPLEMENTARY DATA

Supplementary data for this paper are available at *Journal of Petrology* online.

REFERENCES

Anderson, E. M. & Radley, E. G. (1915). The pitchstones of Mull and their genesis. *Quarterly Journal of the Geological Society, London* **71**, 205–215.

Bulau, J. R. (1982). Intergranular fluid distribution in olivine–liquid basalt systems. Ph.D. thesis, Yale University, New Haven, CT, 105 pp.

Bulau, J. R., Waff, H. S. & Tyburczy, J. A. (1979). Mechanical and thermodynamic constraints on fluid distribution in partial melts. *Journal of Geophysical Research* **84**, 6102–6108.

Cmíral, M., Fitz Gerald, J. D., Faul, U. H. & Green, D. H. (1998). A close look at dihedral angles and melt geometry in olivine-basalt aggregates; a TEM study. *Contributions to Mineralogy and Petrology* **130**, 336–345.

Elliott, M. T., Cheadle, M. J. & Jerram, D. A. (1997). On the identification of textural equilibrium in rocks using dihedral angle measurements. *Geology* **25**, 355–358.

Fujii, N., Osamura, K. & Takahashi, E. (1986). Effect of water saturation on the distribution of partial melt in the olivine–pyroxene–plagioclase system. *Journal of Geophysical Research* **91**, 9253–9259.

Harker, D. & Parker, E. R. (1945). Grain shape and grain growth. *Transactions of the American Society of Metals* **34**, 156–195.

Herring, C. (1951*a*). Surface tension as a motivation for sintering. In: Kingston, W. E. (ed.) *Physics of Powder Metallurgy*. New York: McGraw–Hill, pp. 143–179.

Herring, C. (1951*b*). Some theorems on the free energies of crystal surfaces. *Physical Review* **82**, 87–93.

Holness, M. B. (1993). Temperature and pressure dependence of quartz–aqueous fluid dihedral angles: the control of adsorbed H_2O on the permeability of quartzites. *Earth and Planetary Science Letters* **117**, 363–377.

Holness, M. B. (1995). The effect of feldspar on quartz–H_2O–CO_2 dihedral angles at 4 kbar, with consequences for the behaviour of aqueous fluids in migmatites. *Contributions to Mineralogy and Petrology* **118**, 356–364.

Holness, M. B. & Bunbury, J. M. (2006). Insights into continental rift-related magma chambers: igneous nodules from the Kula Volcanic Terrane, Western Turkey. *Journal of Volcanological and Geothermal Research* (in press).

Holness, M. B. & Lewis, S. (1997). The structure of the halite–brine interface inferred from pressure and temperature variations of

equilibrium dihedral angles in the H_2O–CO_2–halite system. *Geochimica et Cosmochimica Acta* **61**, 795–804.

Holness, M. B., Cheadle, M. J. & McKenzie, D. (2005). On the use of changes in dihedral angle to decode late-stage textural evolution in cumulates. *Journal of Petrology* **46**, 1565–1583.

Hunter, R. H. & McKenzie, D. (1989). The equilibrium geometry of carbonate melts in rocks of mantle composition. *Earth and Planetary Science Letters* **92**, 347–356.

Ikeda, S., Toriumi, M., Yoshida, H. & Ichiko, S. (2002). Experimental study of the textural development of igneous rocks in the late stage of crystallisation: the importance of interfacial energies under non-equilibrium conditions. *Contributions to Mineralogy and Petrology* **142**, 397–415.

Jurewicz, S. R. & Jurewicz, A. J. G. (1986). Distribution of apparent angles on random sections, with emphasis on dihedral angle measurements. *Journal of Geophysical Research* **91**, 9277–9282.

Jurewicz, S. R. & Watson, E. B. (1985). Distribution of partial melt in a felsic system: the importance of surface energy. *Contributions to Mineralogy and Petrology* **85**, 25–29.

Kretz, R. (1966). Interpretation of the shape of mineral grains in metamorphic rocks. *Journal of Petrology* **7**, 68–94.

Laporte, D. (1994). Wetting behaviour of partial melts during crustal anatexis: the distribution of hydrous silicic melts in polycrystalline aggregates of quartz. *Contributions to Mineralogy and Petrology* **116**, 486–499.

Laporte, D. & Provost, A. (2000*a*). Equilibrium geometry of a fluid phase in a polycrystalline aggregate with anisotropic surface energies: dry grain boundaries. *Journal of Geophysical Research* **105**, 25937–25953.

Laporte, D. & Provost, A. (2000*b*). The grain-scale distribution of silicate, carbonate and metallosulphide partial melts: a review of theory and experiments. In: Bagdassarov, N., Laporte, D. & Thompson, A. B. (eds) *Physics and Chemistry of Partially Molten Rocks. Petrology and Structural Geology, 11*. Dordrecht: Kluwer Academic, pp. 93–140.

Laporte, D. & Vielzeuf, D. (1994). Wetting behaviour of partial melts during crustal anatexis: the distribution of hydrous silicic melts in polycrystalline aggregates of quartz. *EOS Transactions, American Geophysical Union* **75**, 364.

Laporte, D. & Watson, E. B. (1995). Experimental and theoretical constraints on melt distribution in crustal sources: the effect of crystalline anisotropy on melt interconnectivity. *Chemical Geology* **124**, 161–184.

Laporte, D., Rapaille, C. & Provost, A. (1997). Wetting angles, equilibrium melt geometry, and the permeability threshold of partially molten crustal protoliths. In: Bouchez, J.-L., Hutton, D. H. & Stephens, W. E. (eds) *Granite: From Segregation of Melt to Emplacement Fabrics*. Norwell, MA: Kluwer Academic, pp. 31–54.

Longhi, J. & Jurewicz, S. R. (1995). Plagioclase–melt wetting angles and textures: implications for anorthosites. *Lunar and Planetary Science* **XXVI**, 859–860.

Lupulescu, A. & Watson, E. B. (1994). Granitic melt connectivity at low-melt fraction in a mafic crustal protolith. *EOS Transactions, American Geophysical Union* **75**, 585–586.

Lupulescu, A. & Watson, E. B. (1995). Tonalitic melt connectivity at low-melt fraction in a mafic crustal protolith at 10 kb and 800°C. *EOS Transactions, American Geophysical Union* **76**, 299–300.

Lupulescu, A. & Watson, E. B. (1999). Low melt fraction connectivity of granitic and tonalitic melts in a mafic crustal rock at 800°C and 1 GPa. *Contributions to Mineralogy and Petrology* **134**, 202–216.

Maclennan, J., McKenzie, D., Gronvold, K., Shimizu, N., Eiler, J. M. & Kitchen, N. (2003). Melt mixing and crystallisation under Theistareykir, northeast Iceland. *Geochemistry, Geophysics Geosystems* **11**(8624), doi:10.1029/2003GC000558.

Maumus, J., Laporte, D. & Schiano, P. (2004). Dihedral angle measurements and infiltration property of SiO_2-rich melts in mantle peridotite assemblages. *Contributions to Mineralogy and Petrology* **148**, 1–12.

McClurg, J. E. (1982). Petrology and evolution of the northern part of the Rhum Ultrabasic Complex. Ph.D. thesis, University of Edinburgh.

Minarik, W. G. & Watson, E. B. (1995). Interconnectivity of carbonate melt at low melt fraction. *Earth and Planetary Science Letters* **133**, 423–437.

Riegger, O. K. & Van Vlack, L. H. W. (1960). Dihedral angle measurement. *Transactions of the Metallurgical Society of the AIME* **218**, 933–935.

Saiki, K., Laporte, D., Vielzeuf, D., Nakashima, S. & Boivin, P. (2003). Morphological analysis of olivine grains annealed in an iron–nickel matrix: experimental constraints on the origin of pallasites and on the thermal history of their parent bodies. *Meteoritics and Planetary Science* **38**, 427–444.

Schäfer, F. N. & Foley, S. F. (2002). The effect of crystal orientation on the wetting behaviour of silicate melts on the surfaces of spinel peridotite minerals. *Contributions to Mineralogy and Petrology*, **143**, 254–261.

Smith, C. S. (1948). Grains, phases and interfaces: an interpretation of microstructure. *Transactions of the Metallurgical Society of the AIME* **175**, 15–51.

Smith, C. S. (1964). Some elementary principles of polycrystalline microstructure. *Metallurgical Reviews* **9**, 1–48.

Toramaru, A. & Fujii, N. (1986). Connectivity of the melt phase in a partially molten peridotite. *Journal of Geophysical Research* **91**, 9239–9252.

Upton, B. G. J., Skovgaard, A. C., McClurg, J., Kirstein, L., Cheadle, M., Emeleus, C. H., Wadsworth, W. J. & Fallick, A. E. (2002). Picritic magmas and the Rum ultramafic complex, Scotland. *Geological Magazine* **139**, 437–452.

Vernon, R. H. (1968). Microstructures of high-grade metamorphic rocks at Broken Hill, Australia. *Journal of Petrology* **9**, 1–22.

Vernon, R. H. (1970). Comparative grain-boundary studies of some basic and ultrabasic granulites, nodules and cumulates. *Scottish Journal of Geology* **6**, 337–351.

Vernon, R. H. (1997). Comment: On the identification of textural disequilibrium in rocks using dihedral angle measurements. By Elliott, M. T. & Cheadle, M. J. *Geology* **25**, 1055.

Vernon, R. H. (1999). Quartz and feldspar microstructures in metamorphic rocks. *Canadian Mineralogist* **37**, 513–524.

Vernon, R. H. (2004). *A Practical Guide to Rock Microstructure*. Cambridge: Cambridge University Press, 594 pp.

Vicenzi, E. P., Rapp, R. P. & Watson, E. B. (1988). Crystal/melt wetting characteristics in partially molten amphibolite. *EOS Transactions, American Geophysical Union* **69**, 482.

von Bargen, N. & Waff, H. S. (1988). Wetting of enstatite by basaltic melt at 1350° and 1·0–2·5 GPa pressure. *Journal of Geophysical Research* **93**, 1153–1158.

Waff, H. S. & Bulau, J. R. (1979). Equilibrium fluid distribution in an ultramafic partial melt under hydrostatic stress conditions. *Journal of Geophysical Research* **84**, 6109–6114.

Walker, D., Jurewicz, S. & Watson, E. B. (1988). Adcumulus dunite growth in a laboratory thermal gradient. *Contributions to Mineralogy and Petrology* **99**, 306–319.

Wanamaker, B. J. & Kohlstedt, D. L. (1991). The effect of melt composition on the wetting angle between silicate melt and olivine. *Physics and Chemistry of Minerals* **18**, 26–36.

Wark, D. A. & Watson, E. B. (1998). Grain-scale permeabilities of texturally equilibrated, monomineralic rocks. *Earth and Planetary Science Letters* **164**, 591–605.

Wark, D. A., Williams, C. A., Watson, E. B. & Price, J. D. (2003). Reassessment of pore shapes in microstructurally equilibrated rocks with implications for permeability of the upper mantle. *Journal of Geophysical Research* **108**(B1), 2050, doi:10.1029/2001JB001575.

Watson, E. B. (1982). Melt infiltration and magma evolution. *Geology* **10**, 236–240.

Watson, E. B., Brenan, J. M. & Baker, D. R. (1990). Distribution of fluids in the continental mantle. In: Menzies, M. A. (ed.) *Continental Mantle*. Oxford: Clarendon, pp. 111–125.

Wulff, G. (1901). Zur Frage der Geschwindigkeit des Wachstums und der Auflosumg der Krystallflachen. *Zeitschrift für Kristallographie und Mineralogie* **34**, 449–530.